

2021

Adaptive Grey-Box Models for Model Predictive Building Control Using the Unscented Kalman Filter

Svenne Freund

Hamburg University of Technology, Germany, svenne.freund@tuhh.de

Gerhard Schmitz

Hamburg University of Technology, Germany

Follow this and additional works at: <https://docs.lib.purdue.edu/ihpbc>

Freund, Svenne and Schmitz, Gerhard, "Adaptive Grey-Box Models for Model Predictive Building Control Using the Unscented Kalman Filter" (2021). *International High Performance Buildings Conference*. Paper 363.

<https://docs.lib.purdue.edu/ihpbc/363>

This document has been made available through Purdue e-Pubs, a service of the Purdue University Libraries. Please contact epubs@purdue.edu for additional information. Complete proceedings may be acquired in print and on CD-ROM directly from the Ray W. Herrick Laboratories at <https://engineering.purdue.edu/Herrick/Events/orderlit.html>

Adaptive Grey-Box Models for Model Predictive Building Control Using the Unscented Kalman Filter

Svenne FREUND^{1*}, Gerhard SCHMITZ¹, Claus Markus TIEMANN¹

¹ Hamburg University of Technology, Institute of Engineering Thermodynamics,
Hamburg, Germany
Phone: +4940 42878-2596, E-mail: svenne.freund@tuhh.de

* Corresponding Author

ABSTRACT

Model predictive control (MPC) for buildings is a promising approach to reduce the energy consumption of buildings while at the same time the thermal user comfort can be improved. The core of this control strategy consists of building models that can describe the thermal behavior of particular zones accurately. Grey-box models are frequently used modeling approaches for control-oriented models, however, these models often have limitations regarding their general applicability. Furthermore, the modeling and identification of models used in MPC still require significant effort and is one of the main obstacles for the actual practical implementation of building predictive control. This paper addresses these issues and presents a framework for the online state and parameter estimation of grey-box models. The results show that (1) this online simultaneous state and parameter estimation highly increases the multi-steps-ahead (up to 48 h) prediction performance, (2) this approach enables the models to adapt to changing environmental conditions and (3) it is possible to use only one pre-defined initial model to describe the thermal behavior of several different zones.

1. INTRODUCTION

Against the background of the environmental impact of energy use, the depletion of primary energy resources and the associated economic consequences, considerable efforts are being made worldwide to realize environmentally-friendly and energy-efficient buildings. According to the European Commission, about 40 % of primary energy demand is related to the building sector (European Commission, 2019). Reducing the energy demand of buildings is therefore of major importance concerning the climate protection goals. Especially in modern buildings with already high energy efficiency standards and a high degree of automation, the control and interaction of the individual building's systems with each other is of decisive importance for the energy efficiency and user comfort of the entire building. This is especially true for non-residential buildings such as large office buildings. The optimization of the building control strategy represents a cost-effective approach compared to other energy-saving measures.

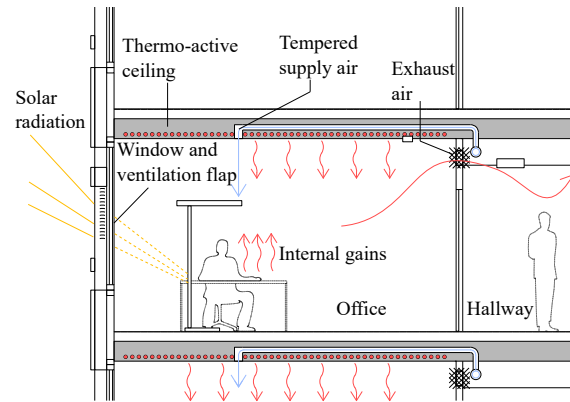
Model predictive control (MPC) of buildings is a promising approach to reduce the energy demand of buildings while improving thermal user comfort (Serale et al., 2018). With the increase in performance and capacity of modern computers and the extensive use of measurement and monitoring systems in buildings, the implementation of advanced, complex control strategies has got more attention in recent years (Sofos et al., 2020). The core of this control strategy consists of one or more simplified and dynamic building models that can describe the thermal behavior of particular zones accurately. Grey-box models based on resistor-capacitor (RC) networks are frequently used modeling approaches for control-oriented models, however, these models often have limitations regarding their general applicability. Furthermore, the modeling and identification of models used in MPC still require significant effort and is one of the main obstacles for the actual practical implementation of building predictive control. This paper addresses these issues and presents a framework for the simultaneous online state and parameter estimation of grey-box models based on an unscented kalman filter (UKF).

1.1 Related Works

To the best of the authors' knowledge, Radecki and Hency (2012) were the first ones who proposed an unscented kalman filter for estimating states and parameters of a thermal RC model. In Radecki and Hency (2013) they compared a UKF-based MPC to thermostat control. The UKF tended to estimate the model parameters to physically impossible values. In those cases, the thermostat control outperformed the MPC. In Radecki and Hency (2017) they tested the



(a) Front view of the investigated building.



(b) Standard single office.

Figure 1: Front view of the office building (a) and schematic of a standard single office (b).

UKF in a one-year-period. Reference measurement data was generated by a detailed white-box model. The root mean square error (RMSE) of a 24 h prediction was 1.48 °C. Maasoumy et al. (2013) used an off-line parameter training to set the initial values for the UKF algorithm. In Martincevic et al. (2014) a method called “clipping” was proposed to prevent the UKF from estimating parameters to physically impossible values. For this purpose, they defined constraints for every parameter by upper and lower boundaries. Every time a parameter value passed the upper or the lower boundary during a filter algorithm step, the value was “clipped” back to the boundary. In Martincevic and Vasak (2019) three additional modifications to the UKF algorithm were added. First, the weighting factors were recalculated after every “clipping” to prevent the mean of the filter’s sigma points from shifting. Second, parameters like the solar irradiance factor were temporarily removed from the augmented state vector when their value did not influence the model output. Third, parameter values were normalized to the interval defined by the upper and lower boundaries to reduce numerical issues. The evaluation of the filter performance with real measurement data resulted in an RMSE of 0.3 °C for a 24 h prediction. Massano et al. (2019) tested the UKF performance on a very simple RC model consisting of one resistor and one capacitor. Reference measurement data was generated by a white-box model. The RMSE of a 24 h prediction was 0.464 °C.

All of the described works neglected the influence of disturbances caused by occupants like the opening of windows or internal gains. The reference data were synthetically generated without disturbances using detail building models. In Alam et al. (2017) disturbances induced by occupants were considered. Alam et al. tested an extended kalman filter to estimate the model states and model parameters for a temporarily occupied living room. Monthly averaged temperature and solar irradiance measurements were used as weather forecast. Several disturbances were considered. The 95th percentile of the absolute prediction error was 1.73 °C in case of a 4 h prediction. Here, the prediction horizon was much smaller while the error value had the same magnitude as in the other papers. Considering more different disturbances can lead to less accurate predictions.

2. BUILDING DESCRIPTION

The office building under investigation, shown in Fig. 1a, is located in Hamburg in Northern Germany. It was designed and built as part of the framework “Energy Optimized Building Construction” (EnOB) as part of the International Building Exhibition in 2013 and serves as the headquarter for the two Local Ministries for Environment and Energy / Urban Development and Housing. Providing a net-floor space of 46 500 m², the building houses 1250 office rooms for around 1500 workplaces. The building can be subdivided into seven low-rise buildings (referred to as building A to D and F to H) with five floors and one 13-story high-rise building (referred to as building E). It was planned and built as a sustainable low-energy building with a target primary energy demand lower than 70 kWh/m²a and a heating demand of around 15 kWh/m²a.

2.1 Standard single office

The majority of office spaces are realized as standard single offices with a rectangular layout. A schematic of a standard single office is shown in Fig. 1b. The basic geometric and construction properties of a single office are given in

Table 1: Basic geometric and construction properties of a single office.

Description	Unit	Value
Width	m	2.5
Clear height	m	2.89
Floor area	m ²	10 to 13
Window area	m ²	2.63
Area of exterior facade (without glazing)	m ²	4.6
Heat transfer coefficient of window	W/m ² K	0.7
Heat transfer coefficient of exterior facade (without glazing)	W/m ² K	0.9

Tab. 1. Each office has a manually openable window and a weather-proofed ventilation flap. The building's envelope is realized as a unitized curtain wall with distinctively colored ceramic panels mounted outside. In winter mode, the offices are mainly heated by thermo-active ceilings (TAC), realized as concrete-core activation with a maximum supply temperature of 32 °C. Mechanical ventilation with preheated air is used to provide the offices with fresh air. During summer mode, the building is passively cooled via the thermo-active ceilings which are fed with chilled water in the range of 18 °C to 20 °C. The building management system (BMS) automatically switches from heating to cooling operation mode based on the averaged outdoor air temperature (OAT) of the past 36 hours. The mechanical ventilation is in summer mode replaced by manual ventilation using the ventilation flaps or windows.

2.2 Heating system

The building's heating system is mainly based on shallow geothermal energy in conjunction with two electrically driven heat pumps, each with a nominal thermal power output of 264 kW. For domestic hot water supply as well as for thermal peak load coverage, a district heating connection is installed. Each building part is separated into two different TAC heating circuits according to the orientation (south/north and south-west/north-east, respectively) resulting in 16 different TAC control loops. The supply temperature set points are gained by a standard linear heating curve using the current outside temperature in combination with a simple heating schedule.

2.3 Monitoring system

To examine the energy demand targets and to consistently optimize the building operation with respect to user comfort and operating costs, a scientific monitoring system was implemented in July 2014. It comprises an extensive network of more than 1100 sensors consisting of various energy meters, flow meters, temperature sensors to measure and record the relevant parameters within the different subsystems with a sample rate of 1 minute. To additionally analyze and evaluate the user comfort, 32 *reference office spaces* were equipped with sensors for air temperature, relative humidity, presence and window handling. These reference offices are mainly office spaces of different orientation, floor plan and floor area and are distributed over the entire building. The measurement data collected with the monitoring system will be used in the presented framework.

3. GREY-BOX MODEL DESCRIPTION

Grey-box models are a trade-off between detailed physical white-box models (standard building simulation software like EnergyPlus or TRNSYS) and purely data-driven black-box models (e. g. neural networks, ARMAX). They have been widely discussed in literature and successfully applied for predictive control strategies. Grey-box models can be represented as networks consisting of thermal resistances R and capacities C . The physical values of those parameters are estimated using suitable identification methods with measured input and output data. Fig. 2 depicts the structure of the here used grey-box model.

The purpose of this model is to describe the thermal behavior (indoor air temperature) of a reference office space adequately. The model consists of seven resistances and four capacities in total (R7C4 model). The four state variables T_W (exterior wall temperature), T_{Air} (indoor air temperature), T_{Int} (temperature of internal masses) and T_{TAC} (TAC temperature) correspond to the four capacities C_W , C_{Air} , C_{Int} and C_{TAC} . Based on available construction data, the initial values for the resistances and capacities are derived and given in Tab. 2. The values for the resistances R_{TAC1} and R_{TAC2} are estimated using the EMPA model developed by (Koschenz & Lehman, 2000).

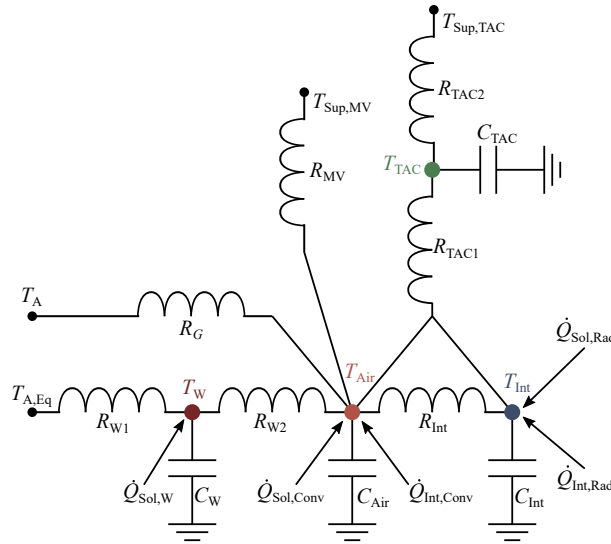


Figure 2: RC-network representation of the used grey-box model.

Table 2: Description and initial values of grey-box model parameters.

Parameter name	Description	Initial value
R_{W1}	Thermal resistance of envelope (exterior side)	0.05 (m ² K)/W
R_{W2}	Thermal resistance of envelope (interior side)	1.11 (m ² K)/W
C_W	Thermal capacitance of envelope	8.5 · 10 ³ J/(m ² K)
R_G	Thermal resistance of glazing	1.43 (m ² K)/W
R_{TAC1}	Thermal resistance between TAC core and zone	0.183 (m ² K)/W
R_{TAC2}	Thermal resistance between TAC core and supply temperature	0.122 (m ² K)/W
C_{TAC}	Thermal capacitance of TAC	7.5 · 10 ⁵ J/(m ² K)
\dot{Q}_{Int}	Internal heat gains	15 W/m ²
R_{Int}	Thermal resistance between room air and internal masses	0.18 (m ² K)/W
C_{Int}	Thermal capacitance of internal masses	1.82 · 10 ⁵ J/(m ² K)
R_{MV}	Thermal resistance of mechanical ventilation	0.15 K/W
f_{Sol}	Effective window area for solar radiation	0.2

The model has in total five inputs: T_A (outdoor air temperature), $T_{Sup,TAC}$ (supply temperature of the corresponding TAC's heating circuit), $T_{Sup,MV}$ (supply temperature of mechanical ventilation), $I_{G,\{N,S,W,E\}}$ (global solar radiation on the corresponding facade orientation) and OCC (binary occupancy signal measured by presence sensor). For the heat exchange between the building exterior and the environment, a simplified approach based on (VDI 6007, 2015) is implemented using the equivalent OAT $T_{A,Eq}$ defined as:

$$T_{A,Eq} = T_A + I_{G,\{N,S,W,E\}} \cdot \frac{\alpha_F}{\alpha_A} \quad (1)$$

The solar heat gains absorbed by the interior are determined according to:

$$\dot{Q}_{Sol} = f_{Sol} \cdot I_{G,\{N,S,W,E\}} \quad (2)$$

where f_{Sol} is an empirical factor and can be interpreted as an effective window area in which the solar radiation enters. The internal heat gains by persons, lighting or equipment are calculated using the measured occupancy signal OCC multiplied by a constant factor \dot{Q}_{Int} . As shown in Fig. 2, the different heat sources are split into a convective part which is acting on the air volume node and a radiative part which is acting on the interior temperature node. The corresponding parts are chosen as follows: internal gains 60 % radiative, 40 % convective; solar gains 90 % radiative, 10 % convective; heat gains by TAC 80 % radiative, 20 % convective.

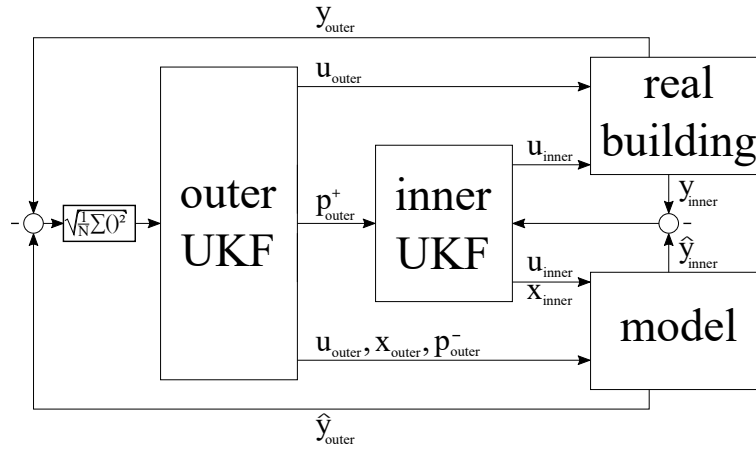


Figure 3: Schematic view of the CUKF operation mode.

The grey-box model, shown in Fig. 2, is implemented in the equation-based, object-oriented modeling language Modelica® (The Modelica Association, 2020). An interface to MATLAB® is developed which enables the manipulation of the parameters and initial states. The following kalman filter algorithm is therefore implemented in MATLAB®.

4. UNSCENTED KALMAN FILTER ALGORITHM

In this study, a combined unscented kalman filter (CUKF) for state and parameter estimation is proposed consisting of two separate unscented kalman filters (UKF), an outer filter and an inner filter. For outer filtering, the grey-box model simulates the room temperature trajectory for the past 48 hours using the available input data. Simultaneously, the measured temperature trajectory of the given time interval is loaded from the record. Simulated and measured trajectories are smoothed by moving mean and moving median filters to reduce disturbance influences like window opening from the data. The outer UKF then estimates the states and parameters of the model by minimizing the RMSE between the smoothed signals. The estimated parameters are then transmitted to the inner filter which estimates the current state of the model. Fig. 3 shows a schematic view of the combined unscented kalman filter operation mode.

A discrete-time non-linear state-space model consisting of the system function $f(\cdot)$ and the measurement function $h(\cdot)$ is considered.

$$\mathbf{x}_k = f(\mathbf{x}_{k-1}, \mathbf{u}_{k-1}) + \boldsymbol{\omega} \quad (3)$$

$$\mathbf{y}_k = h(\mathbf{x}_k) + \mathbf{v} \quad (4)$$

$$\boldsymbol{\omega} \sim \mathcal{N}(0, \mathbf{Q}) \quad (5)$$

$$\mathbf{v} \sim \mathcal{N}(0, \mathbf{R}) \quad (6)$$

$\boldsymbol{\omega}$ and \mathbf{v} are the process noise and the measurement noise with covariance \mathbf{Q} and \mathbf{R} , respectively. They are assumed to be zero mean, gaussian and uncorrelated.

\mathbf{x} is the state vector of the system with covariance matrix \mathbf{P} . For the outer filter $\mathbf{x}_{\text{outer}}$ is an augmented state vector containing the states (temperature levels) $[T_1 \dots T_n]^T$, manipulated parameters $[p_1 \dots p_m]^T$ and the RMSE of the past 48 hours e_{RMSE} . For the inner filter $\mathbf{x}_{\text{inner}}$ is a vector containing only the states $[T_1 \dots T_n]^T$.

$$\mathbf{x}_{\text{outer}} = \begin{bmatrix} T_1 \\ \vdots \\ T_n \\ p_1 \\ \vdots \\ p_m \\ e_{\text{RMSE}} \end{bmatrix}, \quad \mathbf{x}_{\text{inner}} = \begin{bmatrix} T_1 \\ \vdots \\ T_n \end{bmatrix}$$

For initializing the state vector, the parameter values are either obtained by an off-line parameter training or by using the initial values from Tab. 2. The room air temperature T_{Air} is set by the latest measured indoor air temperature value. The other states are initialized as follows: $T_{\text{W}} = 295.15 \text{ K}$, $T_{\text{Int}} = 295.15 \text{ K}$, $T_{\text{TAC}} = 296.15 \text{ K}$. e_{RMSE} is set to zero and the initial state covariance matrix \mathbf{P}_0^+ is set to $\mathbf{P}_0^+ = \mathbf{Q}$.

The general operation mode of the UKF is divided into two steps, prediction step and correction step. In the prediction step a defined number of states, so called sigma points, are generated:

$$\boldsymbol{\chi}_{k-1}^{(0)} = \hat{\mathbf{x}}_{k-1}^+ \quad (7)$$

$$\boldsymbol{\chi}_{k-1}^{(i)} = \hat{\mathbf{x}}_{k-1}^+ + \left(\sqrt{(n + \kappa) \mathbf{P}_{k-1}^+} \right)_i^T, \quad i = 1, \dots, n \quad (8)$$

$$\boldsymbol{\chi}_{k-1}^{(n+i)} = \hat{\mathbf{x}}_{k-1}^+ - \left(\sqrt{(n + \kappa) \mathbf{P}_{k-1}^+} \right)_i^T, \quad i = 1, \dots, n \quad (9)$$

κ is a scaling factor that must fulfill the condition $n + \kappa \neq 0$. The sigma points are then transformed through the system function $f(\cdot)$. This step is called the unscented transform (UT):

$$\boldsymbol{\chi}_k^{(i)} = f\left(\boldsymbol{\chi}_{k-1}^{(i)}, \mathbf{u}_k\right) \quad (10)$$

The RMSE value e_{RMSE} , which is the last entry of the state vector in the outer filter, is defined as the root mean square error between simulated and measured room temperature trajectory:

$$e_{\text{RMSE}}^{(i)} = \sqrt{\frac{1}{N} \sum_{j=1}^N (\hat{T}_j - T_{j,\text{meas.}})^2}, \quad (11)$$

where N is the number of simulated and measured temperature samples. The weighting factors

$$W_m^{(0)} = \frac{\kappa}{n + \kappa} \quad (12)$$

$$W_c^{(0)} = \frac{\kappa}{n + \kappa} + (1 + \beta - \alpha^2) \quad (13)$$

$$W_m^{(i)} = W_c^{(i)} = \frac{1}{2(n + \kappa)}, \quad i = 2, \dots, 2n \quad (14)$$

are used to calculate mean and covariance of the transformed sigma points receiving the *a priori* estimation $\hat{\mathbf{x}}_k^-$ and \mathbf{P}_k^- . α and β are scaling factors. α is usually set to a small value between 0 and 1. β is usually set to 2 when a gaussian distribution is assumed (Julier, 2002).

$$\hat{\mathbf{x}}_k^- = \sum_{i=0}^{2n} W_m^{(i)} \boldsymbol{\chi}_k^{(i)} \quad (15)$$

$$\mathbf{P}_k^- = \sum_{i=0}^{2n} W_c^{(i)} \left(\hat{\mathbf{x}}_k^- - \boldsymbol{\chi}_k^{(i)} \right) \left(\hat{\mathbf{x}}_k^- - \boldsymbol{\chi}_k^{(i)} \right)^T + \mathbf{Q} \quad (16)$$

The transformed sigma points are then transformed again through the measurement function $h(\cdot)$:

$$\mathcal{Y}_k^{(i)} = h\left(\boldsymbol{\chi}_k^{(i)}\right) = \mathbf{H} \boldsymbol{\chi}_k^{(i)} \quad (17)$$

The output matrix \mathbf{H} is defined differently for the inner and the outer UKF. The measurement matrix of the inner filter returns only the estimation of the current indoor air temperature, while the measurement matrix of the outer filter returns air temperature estimation and the RMSE of the estimated temperature trajectory.

$$\mathbf{H}_{\text{inner}} = [1 \quad 0 \quad \dots \quad 0], \quad \mathbf{H}_{\text{outer}} = \begin{bmatrix} 1 & 0 & \dots & 0 & 0 \\ 0 & 0 & \dots & 0 & 1 \end{bmatrix}$$

The *a priori* measurement prediction is received by calculating mean and covariance after the second transformation:

$$\hat{\mathbf{y}}_k = \sum_{i=0}^{2n} W_m^{(i)} \mathcal{Y}_k^{(i)} \quad (18)$$

$$\mathbf{P}_{\mathbf{y},k} = \sum_{i=0}^{2n} W_c^{(i)} \left(\hat{\mathbf{y}}_k - \mathcal{Y}_k^{(i)} \right) \left(\hat{\mathbf{y}}_k - \mathcal{Y}_k^{(i)} \right)^T + \mathbf{R} \quad (19)$$

In the correction step the *a priori* estimation is turned into an *a posteriori* estimation by calculating the cross-covariance matrix $\mathbf{P}_{\mathbf{xy},k}$ and the kalman gain \mathbf{K}_k . For further details about the UKF algorithm see (Simon, 2006).

$$\mathbf{P}_{\mathbf{xy},k} = \sum_{i=0}^{2n} W_c^{(i)} \left(\hat{\mathbf{x}}_k^- - \boldsymbol{\chi}_k^{(i)} \right) \left(\hat{\mathbf{y}}_k - \mathcal{Y}_k^{(i)} \right)^T \quad (20)$$

$$\mathbf{K}_k = \mathbf{P}_{\mathbf{xy}} \mathbf{P}_y^{-1} \quad (21)$$

$$\hat{\mathbf{x}}_k^+ = \hat{\mathbf{x}}_k^- + \mathbf{K}_k (\mathbf{z}_k - \hat{\mathbf{y}}_k) \quad (22)$$

$$\mathbf{P}_k^+ = \mathbf{P}_k^- - \mathbf{K}_k \mathbf{P}_y \mathbf{K}_k^T \quad (23)$$

The measurement vector \mathbf{z}_k only returns the current measured room temperature value in the case of inner filtering and an additional zero entry for the RMSE in the case of outer filtering:

$$\mathbf{z}_{k,\text{inner}} = [T_{k,\text{meas.}}], \quad \mathbf{z}_{k,\text{outer}} = \begin{bmatrix} T_{k,\text{meas.}} \\ 0 \end{bmatrix}$$

The zero entry is needed for the outer filter to minimize the RMSE in every filtering step.

5. RESULTS AND DISCUSSION

In this section, two different applications of the proposed filter algorithm are presented. First, the adaption of a “trained model” to changing environmental and operational conditions is investigated. The second use-case is the online simultaneous parameter and state estimation of an “initial model” without pre-trained parameters. The filter performance is evaluated using the RMSE between the predicted and measured room temperatures for a prediction horizon of 48 hours.

5.1 Adaption to changing system operation

As described, the performance of the CUKF with a pre-trained model under changing system operations is investigated. The parameters of this trained model are estimated with input data from a heating period exclusively. The details of the off-line parameter identification are beyond the scope of this paper. More information can be found in Freund and Schmitz (2019). Furthermore, only the four most influential (defined by parameter sensitivity concerning the simulated room temperature) parameters are set to be manipulable by the filter. The OAT and TAC’s supply temperature of the investigated 30-day-period are shown in Fig. 4a. The system operation changes from a 14-day heating period to a 7-day cooling period and then back to heating operation. As described in Section 2.2, the TACs are also used for passive cooling of the building with a supply temperature of 18 °C to 20 °C. The outdoor air temperature in the considered period varies in a range of 0 °C to 25 °C.

Fig. 4b depicts the measured room air temperature and the one-step-ahead prediction of the model with and without using the CUKF. It appears that the error between measurement and prediction without filter increases when the OAT rises and the system operation switches to cooling mode. This indicates that the initial parameters from the off-line identification step using training data from heating periods are not suitable for significantly changed environmental and operational conditions. Applying the proposed CUKF does improve temperature tracking considerably (Fig. 4b). As described, the filter algorithm updates the states and parameters recursively every 30 minutes using the current measured room temperature and the trajectory from the past 48 hours. Fig. 4c shows the distribution of the RMSE for the 48 hours prediction. Without using any filter, 50 % of the prediction errors are in a range of 0.4 °C to 0.8 °C with a median of 0.56 °C. Using a UKF only for state estimation, the prediction RMSEs drop to a median of 0.4 °C and the distribution is getting significantly narrower. By using the combined state and parameter UKF, the median RMSE can further be reduced to 0.32 °C. In Fig. 4d, the evolution of states and parameters over time are depicted.

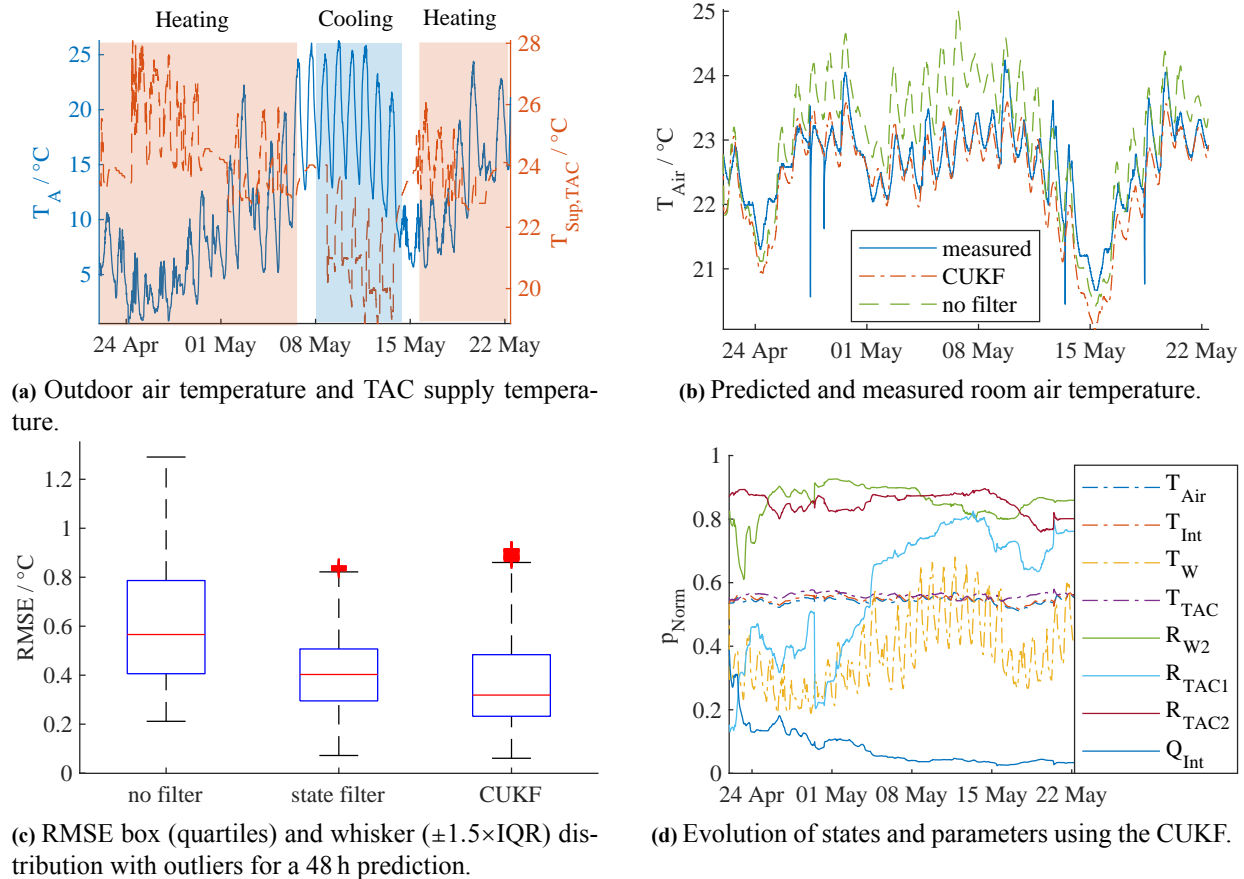


Figure 4: Online parameter and state estimation of a pre-trained model to changing external and operational conditions.

The values are normalized concerning their upper and lower bounds. As shown, all parameters evolve over time and do not converge to a steady-state value. However, the parameter R_{TAC2} (solid light blue curve) indicates a strong correlation to the environmental and operational conditions, as it is increasing distinctly during the cooling period. Overall, the proposed CUKF tunes the parameters and states in a reliable way such that the prediction errors can be reduced significantly and the grey-box model is able to adapt to strongly varying conditions.

5.2 Adaption of an initial model

In the second use-case, the adaption of an initial model without any prior off-line parameter identification step is investigated. The initial parameters of the model, given in Tab. 2, are derived from available construction data and relevant standards. A test period of 28 days during the heating season is chosen. As shown in Fig. 5a, the OAT is in a range of $-3\text{ }^{\circ}\text{C}$ to $12\text{ }^{\circ}\text{C}$ and the TAC supply temperature reaches a maximum of $30\text{ }^{\circ}\text{C}$.

The comparison between the simulated and the measured room temperature, see Fig. 5b, reveals that the initial set of parameters already results in a good agreement. This is emphasized by a low median prediction RMSE of $0.36\text{ }^{\circ}\text{C}$, see Fig. 5c. Applying a UKF for state estimation only does again improve the prediction performance and decreases the median RMSE to $0.26\text{ }^{\circ}\text{C}$. However, by using the CUKF the prediction errors can further be reduced considerably to a median RMSE of $0.19\text{ }^{\circ}\text{C}$ while 50% of the data are in a range of $0.12\text{ }^{\circ}\text{C}$ to $0.28\text{ }^{\circ}\text{C}$. As before, the parameter values evolve constantly over time and do not converge to a steady-state value, see Fig. 5d. This behavior may result from the presence of significant unmeasured disturbances in the used input data. It is quite reasonable that there is not just one optimal set of parameters, but rather a variety of locally optimal parameter sets. Similar behavior can be observed in off-line parameter identification procedures, see Brastein et al. (2018).

To further confirm the results found, the CUKF is applied to five additional reference offices rooms located in the same building sector using the identical initial parameter set and the same 28 days test period. The median values of the

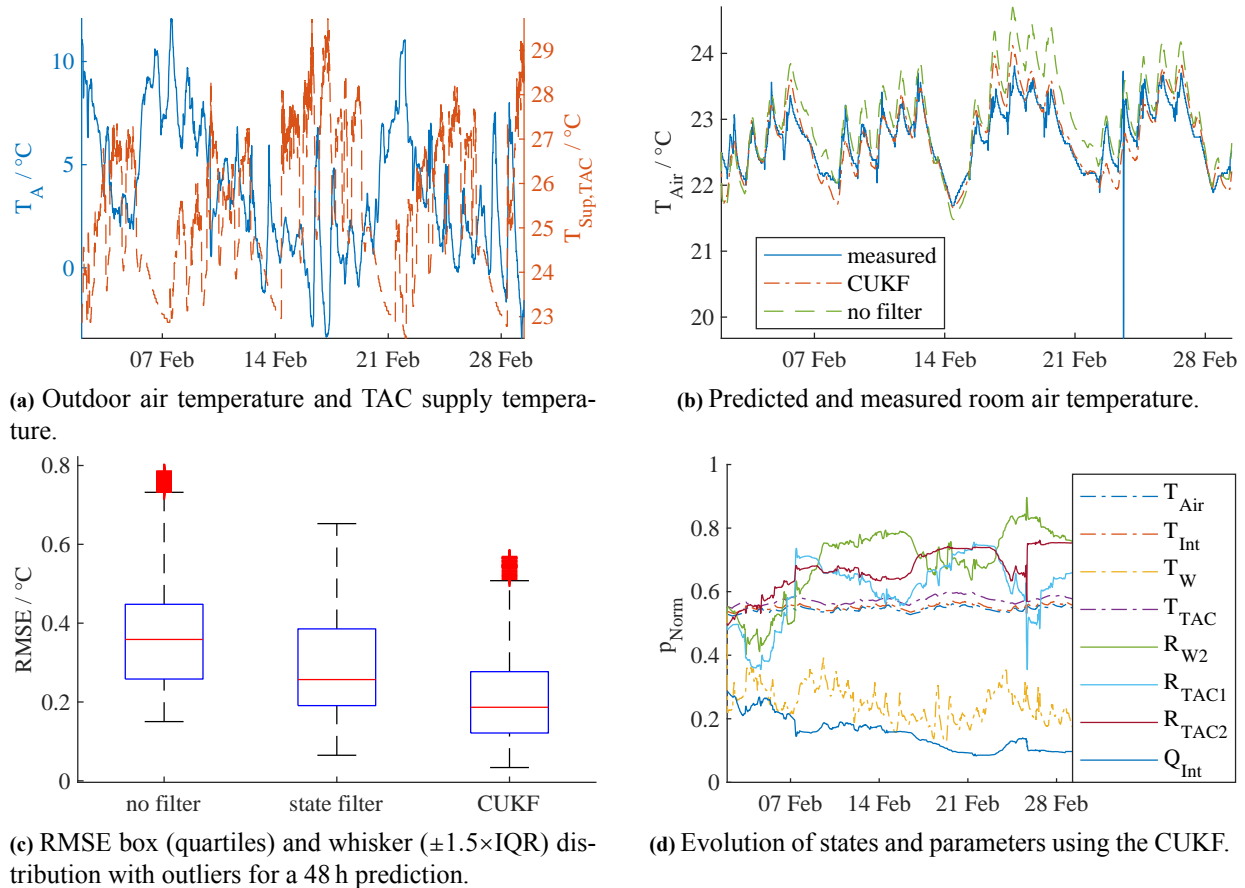


Figure 5: Online parameter and state estimation of an untrained model.

RMSE for the 48 hours prediction are given in Tab. 3. As can be seen, the online combined state and parameter estimation highly increases the prediction performance of all reference rooms and in all cases outperforms the pure state estimation. Therefore, it is possible to use only one pre-defined initial model to describe the thermal behavior of several different zones. Thus, the modeling effort to obtain control-oriented models for MPC applications can be reduced considerably.

6. CONCLUSIONS

In this study, a framework for a combined state and parameter identification for grey-box models using an unscented kalman filter is presented. The proposed filter is tested in two different use cases: the adaptation of a pre-trained model to strongly varying external and operational conditions and the online parameter estimation of an untrained model. The results show that the online simultaneous parameter and state estimation highly increases the 48 hours prediction

Table 3: Median RMSE for a 48 hours prediction using no filter, a UKF state filter and the CUKF.

	Orientation	Floor area	RMSE no filter	RMSE state estimation	RMSE CUKF
Reference room 1	South-West	10.22 m ²	0.62 °C	0.59 °C	0.41 °C
Reference room 2	South-West	11.17 m ²	1.30 °C	0.82 °C	0.46 °C
Reference room 3	North-West	10.25 m ²	0.40 °C	0.39 °C	0.22 °C
Reference room 4	South-East	12.61 m ²	0.44 °C	0.34 °C	0.18 °C
Reference room 5	South-East	26.11 m ²	0.38 °C	0.27 °C	0.24 °C

performance. It further enables the models to reliably adapt to changing external conditions. Furthermore, applying the filter algorithm allows using only one pre-defined initial model to describe the thermal behavior of several different zones. In future work, the implementation of the proposed filter in a model predictive control framework which is currently practically investigated in the described building is planned.

REFERENCES

- Alam, M., Rogers, A., Scott, J., Ali, K., & Auffenberg, F. (2017). *Applying extended kalman filters to adaptive thermal modelling*. University of Oxford, Department of Engineering Science.
- Brastein, O. M., Perera, D., Pfeifer, C., & Skeie, N.-O. (2018). Parameter estimation for grey-box models of building thermal behaviour. *Energy and Buildings*, 169, 58–68. doi: 10.1016/j.enbuild.2018.03.057
- European Commission. (2019). *Eu transport in figures: Statistical pocketbook 2019* (Vol. 2019). Luxembourg: Publications Office of the European Union.
- Freund, S., & Schmitz, G. (2019). Development of a framework for model predictive control (mpc) in a large-sized low-energy office building using modelica grey-box models. In *Building simulation 2019: 16th conference of ibpsa, rome, italy*.
- Julier, S. J. (2002). The scaled unscented transformation. In *Proceedings of the 2002 american control conference (iee cat. no.ch37301)* (p. 4555–4559 vol.6). IEEE. doi: 10.1109/ACC.2002.1025369
- Koschenz, M., & Lehman, B. (2000). *Thermoaktive bauteilsysteme tabs* (1. Aufl. ed.). Dübendorf: EMPA Energiesysteme/Haustechnik.
- Maasoumy, M., Moridian, B., Razmara, M., Shahbakhti, M., & Sangiovanni-Vincentelli, A. (2013). Online simultaneous state estimation and parameter adaptation for building predictive control. In *Asme 2013 dynamic systems and control conference*. American Society of Mechanical Engineers. doi: 10.1115/DSCC2013-4064
- Martincevic, A., Starcic, A., & Vasak, M. (2014). Parameter estimation for low-order models of complex buildings. In *Ieee pes innovative smart grid technologies, europe* (pp. 1–6). IEEE. doi: 10.1109/ISGTEurope.2014.7028767
- Martincevic, A., & Vasak, M. (2019). Constrained kalman filter for identification of semiphysical building thermal models. *IEEE Transactions on Control Systems Technology*, 1–8. doi: 10.1109/TCST.2019.2942808
- Massano, M., Macii, E., Patti, E., Acquaviva, A., & Bottaccioli, L. (2019). A grey-box model based on unscented kalman filter to estimate thermal dynamics in buildings. In *Ieee international conference on environment and electrical engineering* (pp. 1–6). doi: 10.1109/EEEIC.2019.8783974
- Radecki, P., & Hancey, B. (2012). Online building thermal parameter estimation via unscented kalman filtering. In *2012 american control conference (acc)* (pp. 3056–3062). IEEE. doi: 10.1109/ACC.2012.6315699
- Radecki, P., & Hancey, B. (2013). Online thermal estimation, control, and self-excitation of buildings. In *52nd ieee conference on decision and control* (pp. 4802–4807). IEEE. doi: 10.1109/CDC.2013.6760642
- Radecki, P., & Hancey, B. (2017). Online model estimation for predictive thermal control of buildings. *IEEE Transactions on Control Systems Technology*, 25(4), 1414–1422. doi: 10.1109/TCST.2016.2587737
- Serale, G., Fiorentini, M., Capozzoli, A., Bernardini, D., & Bemporad, A. (2018). Model predictive control (mpc) for enhancing building and hvac system energy efficiency: Problem formulation, applications and opportunities. *Energies*, 11(3), 631.
- Simon, D. (2006). *Optimal state estimation: Kalman, h ∞ , and nonlinear approaches*. Hoboken, NJ: Wiley-Interscience. Retrieved from <http://site.ebrary.com/lib/alltitles/docDetail.action?docID=10308111> doi: 10.1002/0470045345
- Sofos, M., Langevin, J., Deru, M., Gupta, E., Benne, K. S., Blum, D., ... Widergren, S. (2020). *Innovations in sensors and controls for building energy management: Research and development opportunities report for emerging technologies*. doi: 10.2172/1601591
- The Modelica Association. (2020). *Modelica*. Modelica Association. Retrieved from <https://www.modelica.org/>
- Verein Deutscher Ingenieure. (2015). *Calculation of transient thermal response of rooms and buildings* (No. 6007). Berlin: Beuth Verlag.